Shift of the magnetopause reconnection line to the winter hemisphere under southward IMF conditions: Geotail and MMS observations

N. Kitamura, H. Hasegawa, Y. Saito, I. Shinohara, S. Yokota, T. Nagai, C. J. Pollock, B. L. Giles, T. E. Moore, J. C. Dorelli, et al.

AGU PUBLICATIONS

Geophysical Research Letters

RESEARCH LETTER
10.1002/2016GL069095

Special Section:
First results from NASA's Magnetospheric Multiscale (MMS) Mission

Shift of the magnetopause reconnection line to the winter hemisphere under southward IMF conditions: Geotail and MMS observations

N. Kitamura[1], H. Hasegawa[1], Y. Saito[1], I. Shinohara[1], S. Yokota[1], T. Nagai[2], C. J. Pollock[3,4], B. L. Giles[3], T. E. Moore[3], J. C. Dorelli[3], D. J. Gershman[3,5], L. A. Avanov[3], W. R. Paterson[3], V. N. Coffey[6], M. O. Chandler[6], J. A. Sauvaud[7], B. Lavraud[7], R. B. Torbert[8], C. T. Russell[9], R. J. Strangeway[9], and J. L. Burch[10]

[1]Institute of Space and Astronautical Science, Japan Aerospace Exploration Agency, Sagamihara, Japan, [2]Tokyo Institute of Technology, Tokyo, Japan, [3]NASA Goddard Space Flight Center, Greenbelt, Maryland, USA, [4]Denali Scientific, Healy, Alaska, USA, [5]Oak Ridge Associated Universities, Washington, District of Columbia, USA, [6]NASA Marshall Space Flight Center, Huntsville, Alabama, USA, [7]Institut de Recherche en Astrophysique et Planétologie (IRAP), Toulouse, France, [8]Space Science Center, University of New Hampshire, Durham, New Hampshire, USA, [9]Institute of Geophysics and Planetary Physics, University of California, Los Angeles, California, USA, [10]Southwest Research Institute, San Antonio, Texas, USA

Key Points:
- The magnetopause reconnection line shifts to the winter hemisphere under southward IMF conditions
- The reconnection line was 1.8 R_E or further northward of GSM Z = 0 plane for IMF By = Bz = −4 nT
- For purely southward IMF, the reconnection line was northward of GSM Z~2 R_E at GSM Y = −6.5 R_E

Correspondence to:
N. Kitamura,
kitamura@stp.isas.jaxa.jp

Citation:
Kitamura, N., et al. (2016), Shift of the magnetopause reconnection line to the winter hemisphere under southward IMF conditions: Geotail and MMS observations, *Geophys. Res. Lett.*, *43*, 5581–5588, doi:10.1002/2016GL069095.

Received 11 APR 2016
Accepted 13 MAY 2016
Accepted article online 18 MAY 2016
Published online 6 JUN 2016

Abstract At 02:13 UT on 18 November 2015 when the geomagnetic dipole was tilted by −27°, the MMS spacecraft observed southward reconnection jets near the subsolar magnetopause under southward and dawnward interplanetary magnetic field conditions. Based on four-spacecraft estimations of the magnetic field direction near the separatrix and the motion and direction of the current sheet, the location of the reconnection line was estimated to be ~1.8 R_E or further northward of MMS. The Geotail spacecraft at GSM Z~1.4 R_E also observed southward reconnection jets at the dawnside magnetopause 30–40 min later. The estimated reconnection line location was northward of GSM Z~2 R_E. This crossing occurred when MMS observed purely southward magnetic fields in the magnetosheath. The simultaneous observations are thus consistent with the hypothesis that the dayside magnetopause reconnection line shifts from the subsolar point toward the northern (winter) hemisphere due to the effect of geomagnetic dipole tilt.

1. Introduction

Under southward interplanetary magnetic field (IMF) conditions, the IMFs reconnect with the terrestrial magnetic fields at the magnetopause in the subsolar to flank regions [e.g., *Dungey*, 1961]. Recent satellite observations have proved that the reconnection line extends across a wide range of local times [e.g., *Phan et al.*, 2006; *Dunlop et al.*, 2011]. Global modeling studies [*Russell et al.*, 2003; *Park et al.*, 2006; *Cnossen et al.*, 2012; *Hoilijoki et al.*, 2014; *Komar et al.*, 2015] have indicated that the location of the dayside magnetopause reconnection line under southward IMF conditions tends to shift toward the winter hemisphere from the subsolar point due to the effect of geomagnetic dipole tilt. *Komar et al.* [2015] surveyed spatial distributions of the magnetic shear angle, the asymmetric outflow speed, the reconnecting component's magnetic energies, and the magnitude of the current density in their global model as candidates that determine the location of the reconnection line, and identified that the maxima of them shift from the subsolar point toward the winter hemisphere.

The modeling result by *Cnossen et al.* [2012] indicated that the total potential drop along the dayside reconnection line, which maps down to the polar caps via magnetic field lines, near solstices (large dipole tilt) is lower (weaker solar wind-magnetosphere coupling) than that near equinoxes using the same solar wind and purely southward directed IMF condition. Since flows in the magnetosheath diverge from the nose, reconnection at such a shifted reconnection line may be affected by the flow that would have a perpendicular component to the reconnection line. Thus, clarifying the location of the magnetic reconnection line at the magnetopause is important to understand the coupling between the solar wind and the magnetosphere.

By estimating the distance to the reconnection site based on time-of-flight effect of precipitating ions in the cusp observed by the Polar spacecraft, *Trattner et al.* [2007] showed that the shift of the magnetopause reconnection line can occur. Recently, direct observations at the magnetopause provided the results consistent with this hypothesis [*Trenchi et al.*, 2008; *Trattner et al.*, 2012; *Zhu et al.*, 2015].

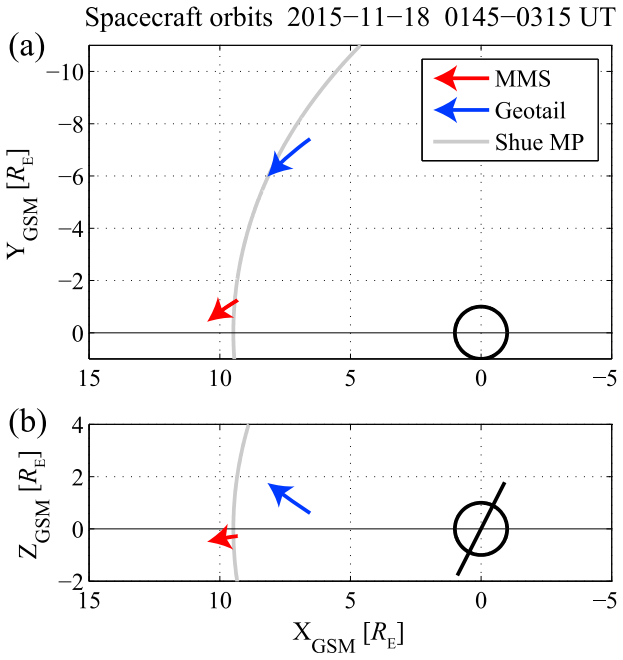

Figure 1. Orbits of the Geotail (blue arrow) and MMS (red arrow) spacecraft in GSM (a) *XY* and (b) *XZ* plane from 01:45 to 03:15 UT on 18 November 2015. Gray curves indicate the magnetopause location from *Shue et al.* [1998] model using the IMF B_z of −5 nT and the solar wind dynamic pressure of 2.5 nPa as the input parameters.

In the present paper, we examine the location of the dayside magnetopause reconnection line under southward IMF conditions using data obtained by the Geotail and MMS (Magnetospheric Multiscale) spacecraft near the GSM $Z = 0$ plane, when the dipole tilt angle was large (−27°) (Figure 1). As discussed later, since the MMS location was close to the subsolar point, the IMF B_y effect on the tilt of the reconnection line [e.g., *Gonzalez and Mozer*, 1974; *Moore et al.*, 2002] would not strongly affect the estimated location of the reconnection line in the subsolar region. Although Geotail was located on the dawnside, the IMF was directed almost purely southward around the magnetopause crossing. Thus, the condition was ideal for investigating the effect of geomagnetic dipole tilt on the latitudinal location of the reconnection line.

2. Data Set

The four MMS spacecraft [*Burch et al.*, 2016] traversed the magnetopause near the subsolar point at (9.7, −1.0, −0.3) R_E in the GSM coordinate system at ~02:13 UT on 18 November 2015 (Figure 1). The magnetic field was measured by the fluxgate magnetometers (FGM) [*Russell et al.*, 2016]. The low-energy ion and electron data were obtained from the Fast Plasma Investigation (FPI) Dual Ion Spectrometer and Dual Electron Spectrometer that can measure three-dimensional distribution functions in an energy range of 0.01–30 keV/q [*Pollock et al.*, 2016]. We mainly use the burst data of low-energy ions (150 ms resolution) and magnetic fields (128 Hz sampling) during the magnetopause crossing.

The Geotail spacecraft [*Nishida*, 1994] crossed the dawnside magnetopause at ~02:50 UT (~40 min after the MMS magnetopause crossing) at (7.7, −6.5, 1.4) R_E in GSM (Figure 1). The ion moment data (0.032–39 keV/q) with a temporal resolution of ~11.5 s were obtained from the low energy particle (LEP) experiment [*Mukai et al.*, 1994]. We also mainly use ~3 s (1 spin) averaged magnetic field data from the magnetic field (MGF) experiment [*Kokubun et al.*, 1994].

As information on IMF, we use the magnetic field data obtained by the Wind Magnetic Field Instrument [*Lepping et al.*, 1995] and the fluxgate magnetometer onboard the ARTEMIS-B spacecraft [*Auster et al.*, 2008]. Wind at around (215, −97, 20) R_E in GSM observed the solar wind on the dawn side of the Earth, while ARTEMIS-B at around (17, 55, −4) R_E in GSM observed that on the dusk side. The solar wind measured by the Wind Solar Wind Experiment [*Ogilvie et al.*, 1995] was steady with a density of ~9 cm^{-3} and a velocity of ~370 km s^{-1} around the time of interest.

3. Observations of the Magnetopause on 18 November 2015

Figures 2a–2c show the data taken by the MMS-3 spacecraft around the magnetopause crossing. Since the separation of the four MMS spacecraft was ~10 km during this event, no differences among the four spacecraft can be seen on this time scale. After 01:59 UT, fast southward ion flows with a speed of >150 km s^{-1} were observed during partial and full magnetopause crossings (Figure 2b). These flow speeds were comparable with or higher than the Alfvén speed in the magnetosheath (~184 km s^{-1}) where the ion density was ~35 cm^{-3} and the magnetic field strength was ~50 nT (Figures 2a and 2c). These fast southward flows indicate that the reconnection line stayed northward of MMS located at GSM $Z = -0.33$ R_E. We perform

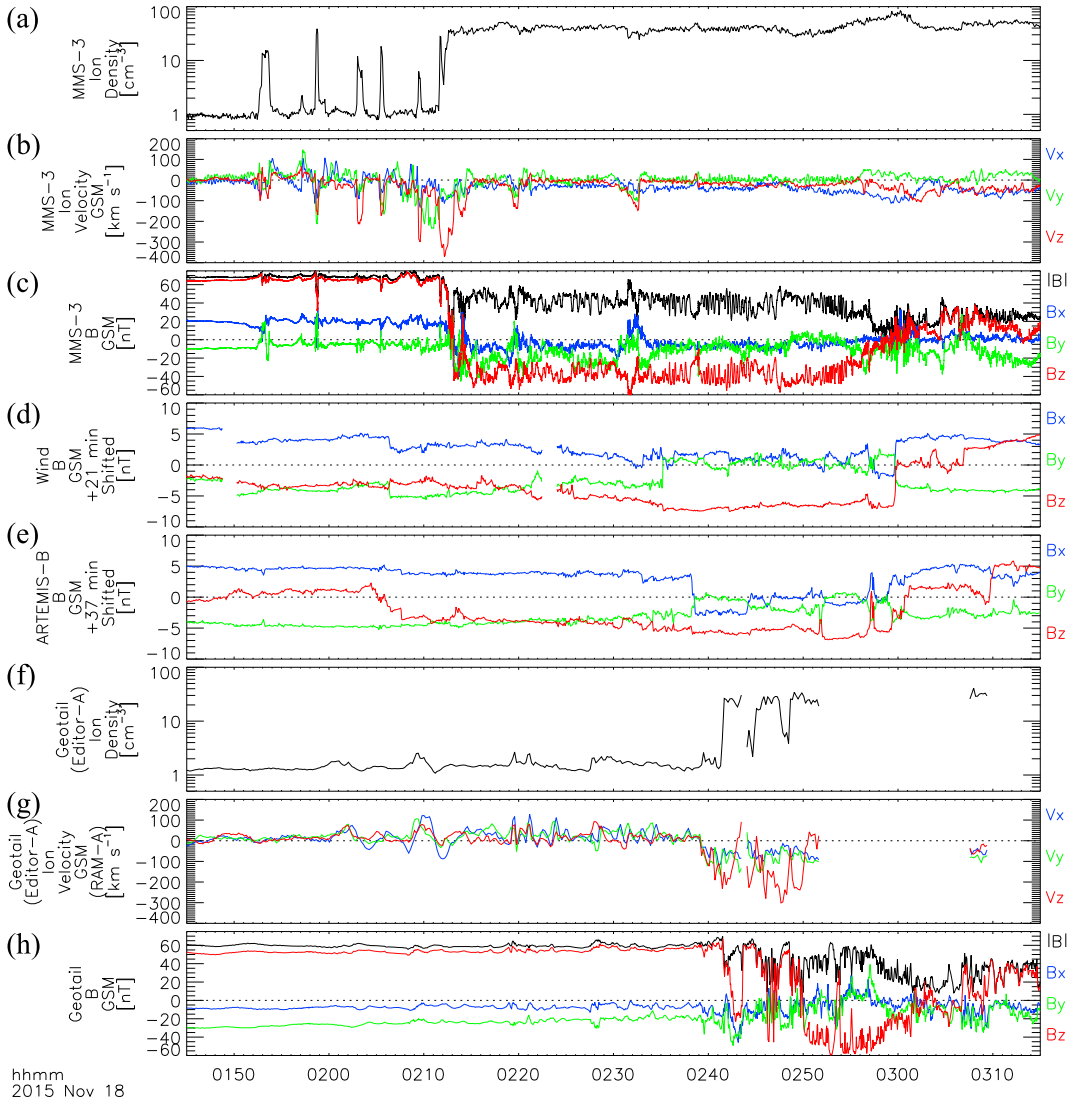

Figure 2. (a) Ion densities, (b) bulk velocities (4.5 s resolution), and (c) magnetic field (16 Hz sampling) observed by the MMS-3 spacecraft, time-shifted IMF observed by (d) the Wind (+21 min) and (e) ARTEMIS-B (+37 min) spacecraft, and (f) ion density, (g) bulk velocity, and (h) magnetic field observed by the Geotail spacecraft for the 90 min interval from 01:45 to 03:15 UT. The magnetic field and ion bulk velocity data are shown in the GSM coordinates. The blue, green, and red curves indicate the *x*, *y*, and *z* components, respectively. The magnitude of magnetic fields is shown as black curves in the plots of magnetic fields observed by MMS-3 and Geotail. Ion density values from Geotail were doubled to take into account saturation of the ion detector in high particle flux region.

more detailed analysis of a full magnetopause crossing at ~02:13 UT in section 4 to estimate the location of the reconnection line.

Time-shifted IMF data obtained from the Wind (+21 min) and ARTEMIS-B (+37 min) spacecraft are shown in Figures 2d and 2e. The time shift of the Wind data is determined using the B_z change from negative values to ~0 that was observed by MMS in the magnetosheath around 03:00 UT. The time shift between the Wind and ARTEMIS-B data is determined using the changes in B_x, B_y, and B_z around 03:00 UT (after the time shift shown in Figure 2). The time-shifted IMF data indicate that the IMF B_z was negative around the time of the MMS full magnetopause crossing. The IMF also had dawnward and sunward components with a magnitude almost equal to the southward one (~4 nT). Since the magnitude of B_y in the magnetosheath was smaller than that of B_z after ~02:16 UT (Figure 2c), the local magnetic field in the magnetosheath was probably dominated by the negative B_z component at the time of the magnetopause crossing. The relatively

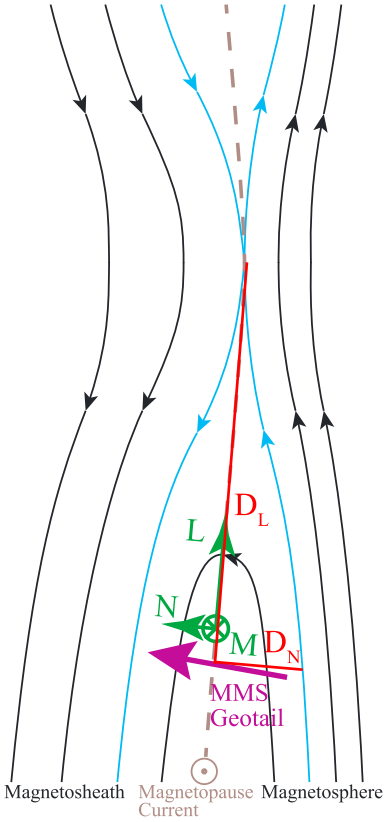

Figure 3. Schematic of the magnetic reconnection at the magnetopause, and LMN coordinates, showing how we estimate the distance D_L from the location of the spacecraft (purple arrow) to the reconnection line based on the magnetic field component ratio in the *LMN* coordinate (B_N/B_L) near the separatrix (blue curves) and the distance D_N between the separatrix and the center of the current sheet (gray dashed curve).

small *y* component of the jet velocity after 02:09 UT was consistent with dominantly southward IMFs [*Trenchi et al.*, 2008].

The ion moment data derived by Geotail around the magnetopause crossing are plotted in Figures 2f–2h. Transitions between low and high ion densities, southward jets (~200 km s^{-1}), and reversals of B_z were detected (around 02:42, 02:46, and 02:49 UT). Data gaps after 02:43 UT in Figures 2f and 2g were caused by changes of the LEP observation mode from RAM-A (normal mode) to RAM-B in which ions at energies below ~5 keV were not measured to protect the detector from large fluxes of low-energy ions in the magnetosheath (and solar wind). Since the main part of magnetosheath ions was not detected in the RAM-B mode, the moment data are not plotted. All of B_z reversals when ions were measured in the RAM-A mode were accompanied by southward jets. This result indicates that magnetopause reconnection occurred northward of Geotail despite its GSM *Z* location of ~1.4 R_E. This northward shift of the reconnection line is consistent with the hypothesis that the reconnection line shifts toward the winter hemisphere owing to the effect of geomagnetic dipole tilt [e.g., *Russell et al.*, 2003; *Park et al.*, 2006].

The time-shifted IMF data indicate that the IMF was almost purely southward around the time of the Geotail magnetopause crossing. Since the magnetic field in the magnetosheath was also almost purely southward (Geotail at 02:50–02:53 and 02:54–03:00 UT (Figure 2h) and MMS (Figure 2c)), the effect of B_y was definitely small. Thus, the northward shift of the reconnection line observed by Geotail would have been purely due to the effect of geomagnetic dipole tilt.

4. MMS-Based Estimation of the Distance to the Reconnection Line

We focus on the period of the full magnetopause crossing from 02:12:05 to 02:13:20 UT. The current densities were estimated using the fast survey magnetic field data (16 Hz sampling) and the curlometer technique [e.g., *Robert et al.*, 1998]. The *N* axis (0.9733, −0.1570, −0.1673 (GSM)) of the *LMN* coordinate system (Figure 3) was defined as the normal to the plane of the magnetopause current sheet that was estimated using the minimum variance analysis of current densities (MVAJ) [*Haaland et al.*, 2004] applied to this period. The positive direction of the *N* axis points outward. The *L* axis (0.1974, 0.2013, 0.9594 (GSM)) was defined as the nearest direction in the plane of the magnetopause current sheet from the maximum variance direction [*Sonnerup and Scheible*, 1998] of magnetic fields measured by all four spacecraft (0.2272, 0.1985, 0.9534 (GSM)). The *M* axis (−0.1170, −0.9669, 0.2269 (GSM)) was defined to close the right handed orthogonal system.

Lee et al. [2014] estimated the distance to the reconnection line using the *N* and *L* components of magnetic fields (B_L and B_N) at the separatrix and the distance between the separatrix and the center of the current sheet (D_N in Figure 3). Although for this magnetopause crossing MMS did not reach the separatrix on the magnetospheric side, around 02:12:05 UT, B_L was almost equal to that in the magnetosphere and the ion density was within a factor of ~2 from the magnetospheric level (~1 cm^{-3}) in Figures 2a and 4c. Thus, we believe that this point was not far from the separatrix. Using B_{L_avg} (an averaged value within ±0.5 s

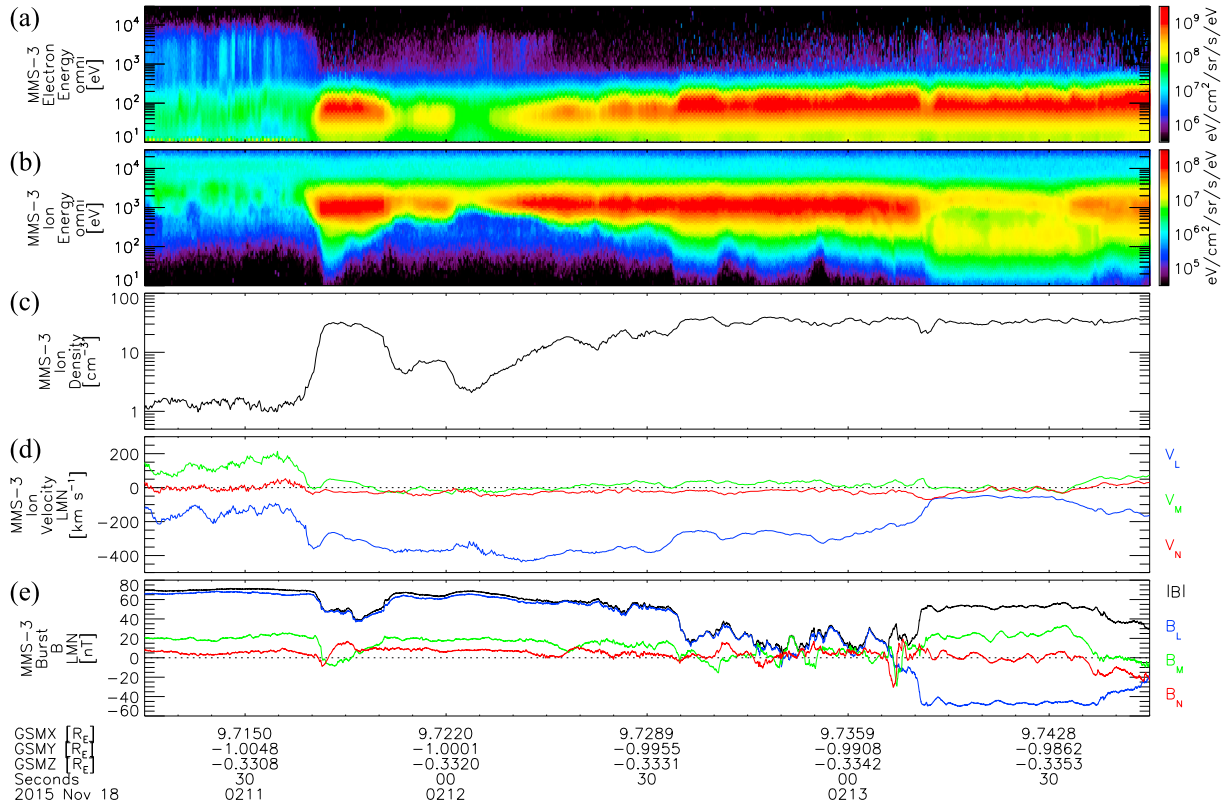

Figure 4. Energy-time spectrograms of (a) electrons and (b) ions, (c) ion density, (d) ion bulk velocity, and (e) magnetic field in LMN coordinates during the full magnetopause crossing observed by the MMS-3 spacecraft. The blue, green, and red curves indicate the *L*, *M*, and *N* components, respectively. The magnitude of magnetic field is shown as black curve in Figure 4e. All data were obtained in the burst mode.

from 02:12:05 UT: 64.6 nT) and B_{N_avg} (an averaged value during this crossing: 3.85 nT), the ratio between the distance to the reconnection line (D_L in Figure 3) and D_N was estimated as 0.060. The lower limit of D_N was estimated as ~800 km, using the *N* component of the deHoffmann-Teller (dHT) velocity (V_{N_dHT}) of $-17.7\ km\ s^{-1}$ and the time period between the nearest point of the magnetospheric separatrix for this crossing (02:12:05 UT) and the center of the current sheet (a minimum of the magnitude of magnetic fields: 02:12:50 UT). The dHT analysis [*Sonnerup et al.*, 1987; *Khrabrov and Sonnerup,* 1998a] was performed using ion velocity and magnetic field data taken by MMS-3 during this magnetopause crossing. Using these estimated D_N (lower limit), B_{N_avg}/B_{L_avg}, and D_N/D_L, the lower limit of D_L was estimated as 2.08 R_E ($D_N/(B_{N\_avg}/B_{L\_avg})$). We calculated dHT velocities and performed the similar analysis using each of the other three MMS spacecraft. The derived lower limit of D_L ranged from 2.08 to 2.13 R_E (Table 1). This D_L corresponds to GSM Z~1.8 R_E, which indicates that the reconnection line was shifted toward the northern (winter) hemisphere from the GSM $Z = 0$ plane.

As a consistency check, we performed the minimum Faraday residue (MFR) analysis [*Khrabrov and Sonnerup*, 1998b] and replaced the *N* axis and the *N* component of the dHT velocity by the normal and velocity (V_{N_MFR}), respectively, of the current sheet that were derived by the MFR analysis. The derived lower limit of D_L was 2.71–4.36 R_E using the data obtained by each of the four MMS spacecraft (Table 1).

The ion spectra had a clear low-energy cutoff from ~02:11:50 UT to 02:12:30 UT. Since this cutoff energy tends to increase before 02:12:03 UT, this change cannot be explained by a temporal effect in which ions are accelerated by reconnection at a certain time and faster (higher energy) ions can reach earlier to a certain distance from the reconnection site [*Zhu et al.*, 2015]. Since the jets were almost always observed around the magnetopause crossing, magnetopause reconnection northward of MMS was probably temporally quasi-continuous. If reconnection is temporally continuous, faster ions can escape

Table 1. Distances to and Locations of the Reconnection Line Estimated From the Combined MVAJ–dHT, MFR, and Ion Dispersion Analyses

	MMS-1	MMS-2	MMS-3	MMS-4	Geotail
Normal in GSM (MVAJ)		(0.9733, −0.1570, −0.1673)			-[a]
B_N (nT)/B_L (nT)		3.85/64.6 = 0.060			-
V_{N_dHT} (km s^{-1})	−17.9	−17.7	−17.7	−18.1	-
D_L (R_E)	>2.11	>2.08	>2.08	>2.13	-
GSM Z (R_E)	>1.77	>1.75	>1.75	>1.80	-
Normal in GSM (MFR)	(0.9828, 0.0189, −0.1840)	(0.9814, −0.0786, −0.1749)	(0.9820, −0.0567, −0.1804)	(0.9804, −0.0829, −0.1786)	(0.8847, −0.4585, −0.0842)
V_{N_MFR} (km s^{-1})	−25.3	−19.6	−20.8	−19.8	−7.99
B_N (nT)/B_L (nT)	2.66/64.7 = 0.041	3.32/64.6 = 0.051	3.03/64.4 = 0.047	3.23/64.5 = 0.050	2.88/42.7 = 0.067
D_L (R_E)	>4.36	>2.71	>3.12	>2.80	>0.5
GSM Z (R_E)	>4.03	>2.38	>2.79	>2.47	>1.9
E_1, E_2 (eV)	800, 580	800, 580	750, 560	750, 580	-[b]
V_{N_in} (dHT) (km s^{-1})	20.7	16.6	19.7	15.9	-
D_L (dHT) (R_E)	1.8	2.3	2.0	3.3	-
GSM Z (dHT) (RE)	1.5	2.0	1.7	3.0	-
V_{N_in} (MFR) (km s^{-1})	12.2	11.1	12.6	10.3	-
D_L (MFR) (R_E)	4.4	3.7	3.7	5.5	-
GSM Z(MFR) (R_E)	4.1	3.4	3.4	5.2	-

[a]MVAJ cannot be performed only using single spacecraft data.
[b]Ion dispersion could not be identified from the Geotail LEP data.

along the reconnected magnetic field lines nearer to the separatrix, while slower ions drift away from the separatrix toward the center of the current sheet. Thus, if one can derive change of the low-energy cutoff and the drift velocity, the distance to the reconnection line can be estimated using the following equation [*Nakamura et al.*, 1998]:

$$D_L \sim \frac{(t_2 - t_1)V_N}{V_{N\_in}} \frac{V_1 V_2}{V_2 - V_1}, \quad (1)$$

where V_N is the N component of the velocity of the magnetopause current sheet, V_{N_in} is the N component of the inflow velocity toward the center of the current sheet in the frame of the N component of the dHT velocity (V_{N_in} (dHT)) or in the frame of the velocity of the current sheet (V_{N_in} (MFR)), and V_1 and V_2 are the ion velocity at the low-energy cutoff at t_1 and t_2, respectively. The low-energy cutoff of ions with pitch angles of ~180° was monotonically decreased from ~750 eV (E_1) at 02:12:06 UT (t_1) to ~560 eV (E_2) at 02:12:12 UT (t_2) (MMS-3). These energies (E_1 and E_2) were converted to ion velocities (V_1 and V_2) using the mass of protons. Using averages of V_{N_in} (V_{N_in} (dHT): 19.7 km s^{-1} and V_{N_in} (MFR): 12.6 km s^{-1}), D_L was estimated as 2.0 and 3.7 R_E, respectively. We estimate D_L as 1.8–5.5 R_E using data from other spacecraft (Table 1). Although the variability of the estimated D_L is fairly large, the distance is consistent with the result in the first half of this section on average. The large variability is partly due to the very limited time length that is usable for this analysis.

5. Geotail-Based Estimation of the Distance to the Reconnection Line

We performed the MFR analysis on Geotail data for the period of 02:49:30–02:51:12 UT. For the MFR analysis, we use ~11.5 s (4 spin) averaged MGF data that have the same temporal resolution as the ion moment data. The normal (N axis) and velocity of the current sheet were derived by the MFR analysis (Table 1). The L, M, and N axis ((0.1342, 0.0776, 0.9879), (−0.4464, −0.8853, 0.1302), (0.8847, −0.4585, −0.0842)) were determined by the same method as applied to the MMS magnetopause crossing. A maximum of B_L (42.7 nT) at 02:49:32 UT was regarded as the nearest point of the magnetospheric separatrix for this crossing. Using this B_L and B_{N_avg} (an averaged value during this crossing: 2.88 nT), D_N/D_L was estimated as 0.067. The lower limit of D_N was estimated as ~200 km, using the N component of the velocity of the current sheet (−7.99 km s^{-1}) and the time period between the nearest point of the magnetospheric separatrix for this crossing (02:49:32 UT) and the center of the current sheet (a reversal of B_L: 02:49:57 UT). We derived D_L as 0.5 R_E corresponding to a reconnection site at GSM $Z > 1.9$ R_E (Table 1).

6. Discussion

B_N/B_L is equivalent to the dimensionless reconnection rate. The derived B_N/B_L ranged between 0.041 and 0.067. They are within the range of other spacecraft observations of B_N/B_L or the reconnection rate estimated by other methods at the magnetopause (most of them were 0.01–0.1) [*Vaivads et al.*, 2004; *Mozer and Retinò*, 2007; *Fuselier et al.*, 2010; *Wang et al.*, 2015].

Owing to a large Alfvén Mach number of the solar wind (8–9), the effect of the IMF B_x is not expected to be large [*Peng et al.*, 2010]. For the MMS magnetopause crossing, the effect of IMF B_y (tilt of the reconnection line) [e.g., *Gonzalez and Mozer*, 1974; *Moore et al.*, 2002] probably contributed to the northward shift of the reconnection line, since the IMF B_y was negative and the MMS magnetopause crossing occurred in the dawnside of the subsolar point. However, near the reconnection site, the direction of the jet tends to be nearly perpendicular to the reconnection line [*Trenchi et al.*, 2008]. Considerably small magnitude of V_y as compared to $-V_z$ in the jet near the MMS full magnetopause crossing (Figure 2b) implies that the tilt of the reconnection line was small. Furthermore, since the position of the MMS was only ~1 R_E away from the subsolar point and IMF B_z was almost comparable with IMF B_y (clock angle~230°), the tilt of the reconnection line was not sufficient to fully explain the northward shift at the MMS location of the reconnection line.

In the Phase-1B of the mission, MMS will be able to observe the magnetopause only up to GSM Z~2 at near-noon local times [*Fuselier et al.*, 2016]. Thus, there may be limited chances to observe diffusion regions of magnetopause reconnection in the subsolar region under southward IMF conditions due to the effect of the dipole tilt.

7. Conclusions

We examined the location of the dayside magnetopause reconnection line using the data obtained by the Geotail and MMS spacecraft near the GSM $Z = 0$ plane under southward IMF and largely tilted geomagnetic dipole conditions.

The observations by MMS and Geotail strongly support the hypothesis that the dayside magnetopause reconnection line shifts toward the northern (winter) hemisphere under southward IMF conditions. Especially around the magnetopause crossing by Geotail, the estimated GSM Z location of the reconnection line was larger than ~2 R_E under almost purely southward IMF, which was unambiguously measured by all of the Geotail (after the magnetopause crossing), Wind, ARTEMIS-B, and MMS spacecraft. Also for the magnetopause crossing by MMS when the IMF B_x and B_y may have only slightly affected the northward shift of the reconnection line, the estimated GSM Z location of the reconnection line was larger than ~1.8 R_E. The shift cannot be explained by any effect other than the dipole tilt, although further study, especially comparison with global modeling studies, is necessary to clarify which of the local parameters that are affected by the dipole tilt determines the location of the reconnection line.

Acknowledgments
The Geotail data are available from DARTS (https://darts.isas.jaxa.jp/stp/geotail/). Wind data were obtained from CDAweb (http://cdaweb.gsfc.nasa.gov/). We acknowledge Vassilis Angelopoulos for use of ARTEMIS data. We acknowledge Eric Grimes and the developing team of the SPEDAS software for the use. IRAP contribution to MMS was supported by CNES. MMS Level-2 data (FPI version 2.1.0 and FGM version 4.18.0) are available from the MMS Science Data Center (https://lasp.colorado.edu/mms/sdc/public/).

References

Auster, H. U., et al. (2008), The THEMIS fluxgate magnetometer, *Space Sci. Rev.*, *141*, 235–264, doi:10.1007/s11214-008-9365-9.
Burch, J. L., T. E. Moore, R. B. Torbert, and B. L. Giles (2016), Magnetospheric multiscale overview and science objectives, *Space Sci. Rev.*, *199*, 5–21, doi:10.1007/s11214-015-0164-9.
Cnossen, I., M. Wiltberger, and J. E. Ouellette (2012), The effects of seasonal and diurnal variations in the Earth's magnetic dipole orientation on solar wind-magnetosphere-ionosphere coupling, *J. Geophys. Res.*, *117*, A11211, doi:10.1029/2012JA017825.
Dungey, J. W. (1961), Interplanetary magnetic field and the auroral zones, *Phys. Rev. Lett.*, *6*, 47–48, doi:10.1103/PhysRevLett.6.47.
Dunlop, M. W., et al. (2011), Magnetopause reconnection across wide local time, *Ann. Geophys.*, *29*, 1683–1697, doi:10.5194/angeo-29-1683-2011.
Fuselier, S. A., S. M. Petrinec, and K. J. Trattner (2010), Antiparallel magnetic reconnection rates at the Earth's magnetopause, *J. Geophys. Res.*, *115*, A10207, doi:10.1029/2010JA015302.
Fuselier, S. A., W. S. Lewis, C. Schiff, R. Ergun, J. L. Burch, S. M. Petrinec, and K. J. Trattner (2016), Magnetospheric multiscale science mission profile and operations, *Space Sci. Rev.*, *199*, 77–103, doi:10.1007/s11214-014-0087-x.
Gonzalez, W. D., and F. S. Mozer (1974), A quantitative model for the potential resulting from reconnection with an arbitrary interplanetary magnetic field, *J. Geophys. Res.*, *79*, 4186–4194, doi:10.1029/JA079i028p04186.
Haaland, S., B. U. Ö. Sonnerup, M. W. Dunlop, E. Georgescu, G. Paschmann, B. Klecker, and A. Vaivads (2004), Orientation and motion of a discontinuity from Cluster curlometer capability: Minimum variance of current density, *Geophys. Res. Lett.*, *31*, L10804, doi:10.1029/2004GL020001.
Hoilijoki, S., V. M. Souza, B. M. Walsh, P. Janhunen, and M. Palmroth (2014), Magnetopause reconnection and energy conversion as influenced by the dipole tilt and the IMF B_x, *J. Geophys. Res. Space Physics*, *119*, 4484–4494, doi:10.1002/2013JA019693.
Khrabrov, A. V., and B. U. Ö. Sonnerup (1998a), DeHoffmann-Teller Analysis, in *Analysis Methods for Multispacecraft Data*, edited by G. Paschmann and P. W. Daly, chap. 9, pp. 221–248, ESA Publ., Noordwijk, Netherlands.

Khrabrov, A. V., and B. U. Ö. Sonnerup (1998b), Orientation and motion of current layers: Minimization of the Faraday residue, *Geophys. Res. Lett.*, *25*, 2372–2376, doi:10.1029/98GL51784.
Kokubun, S., T. Yamamoto, M. H. Acuna, K. Hayashi, K. Shiokawa, and H. Kawano (1994), The Geotail magnetic field experiment, *J. Geomag. Geoelectr.*, *46*, 7–21.
Komar, C. M., R. L. Fermo, and P. A. Cassak (2015), Comparative analysis of dayside magnetic reconnection models in global magnetosphere simulations, *J. Geophys. Res. Space Physics*, *120*, 276–294, doi:10.1002/2014JA020587.
Lee, S. H., H. Zhang, Q.-G. Zong, A. Otto, D. G. Sibeck, Y. Wang, K.-H. Glassmeier, P. W. Daly, and H. Rème (2014), Plasma and energetic particle behaviors during asymmetric magnetic reconnection at the magnetopause, *J. Geophys. Res. Space Physics*, *119*, 1658–1672, doi:10.1002/2013JA019168.
Lepping, R. P., et al. (1995), The Wind magnetic field investigation, *Space Sci. Rev.*, *71*, 207–229, doi:10.1007/BF00751330.
Moore, T. E., M.-C. Fok, and M. O. Chandler (2002), The dayside reconnection *X* line, *J. Geophys. Res.*, *107*(A10), 1332, doi:10.1029/2002JA009381.
Mozer, F. S., and A. Retinò (2007), Quantitative estimates of magnetic field reconnection properties from electric and magnetic field measurements, *J. Geophys. Res.*, *112*, A10206, doi:10.1029/2007JA012406.
Mukai, T., S. Machida, Y. Saito, M. Hirahara, T. Terasawa, N. Kaya, T. Obara, M. Ejiri, and A. Nishida (1994), The low energy particle (LEP) experiment onboard the Geotail satellite, *J. Geomagn. Geoelectr.*, *46*, 669–692.
Nakamura, M., K. Seki, H. Kawano, T. Obara, and T. Mukai (1998), Reconnection event at the dayside magnetopause on 10 January 1997, *Geophys. Res. Lett.*, *25*, 2529–2532, doi:10.1029/98GL00135.
Nishida, A. (1994), The GEOTAIL mission, *Geophys. Res. Lett.*, *21*, 2871–2873, doi:10.1029/94GL01223.
Ogilvie, K. W., et al. (1995), SWE, A comprehensive plasma instrument for the Wind spacecraft, *Space Sci. Rev.*, *71*, 55–77, doi:10.1007/BF00751326.
Park, K. S., T. Ogino, and R. J. Walker (2006), On the importance of antiparallel reconnection when the dipole tilt and IMF B_y are nonzero, *J. Geophys. Res.*, *111*, A05202, doi:10.1029/2004JA010972.
Peng, Z., C. Wang, and Y. Q. Hu (2010), Role of IMF B_x in the solar wind-magnetosphere-ionosphere coupling, *J. Geophys. Res.*, *115*, A08224, doi:10.1029/2010JA015454.
Phan, T. D., H. Hasegawa, M. Fujimoto, M. Oieroset, T. Mukai, R. P. Lin, W. Paterson (2006), Simultaneous Geotail and Wind observations of reconnection at the subsolar and tail flank magnetopause, *Geophys. Res. Lett.*, *33*, L09104, doi:10.1029/2006GL025756.
Pollock, C., et al. (2016), Fast plasma investigation for magnetospheric multiscale, *Space Sci. Rev.*, *199*, 331–406, doi:10.1007/s11214-016-0245-4.
Robert, P., M. W. Dunlop, A. Roux, and G. Chanteur (1998), Accuracy of current density determination, in *Analysis Methods for Multispacecraft Data*, edited by G. Paschmann and P. W. Daly, pp. 395–418, ESA Publ, Noordwijk, Netherlands.
Russell, C. T., Y. L. Wang, and J. Raeder (2003), Possible dipole tilt dependence of dayside magnetopause reconnection, *Geophys. Res. Lett.*, *30*(18), 1937, doi:10.1029/2003GL017725.
Russell, C. T., et al. (2016), The magnetospheric multiscale magnetometers, *Space Sci. Rev.*, *199*, 189–256, doi:10.1007/s11214-014-0057-3.
Shue, J.-H., et al. (1998), Magnetopause location under extreme solar wind conditions, *J. Geophys. Res.*, *103*, 17,691–17,700, doi:10.1029/98JA01103.
Sonnerup, B. U. Ö., and M. Scheible (1998), Minimum and maximum variance analysis, in *Analysis Methods for Multispacecraft Data*, edited by G. Paschmann and P. W. Daly, chap. 8, pp. 185–220, ESA Publ., Noordwijk, Netherlands.
Sonnerup, B. U. Ö., I. Papamastorakis, G. Paschmann, and H. Lühr (1987), Magnetopause properties from AMPTE/IRM observations of the convection electric field: Method development, *J. Geophys. Res.*, *92*, 12,137–12,159, doi:10.1029/JA092iA11p12137.
Trattner, K. J., J. S. Mulcock, S. M. Petrinec, and S. A. Fuselier (2007), Probing the boundary between antiparallel and component reconnection during southward interplanetary magnetic field conditions, *J. Geophys. Res.*, *112*, A08210, doi:10.1029/2007JA012270.
Trattner, K. J., S. M. Petrinec, S. A. Fuselier, and T. D. Phan (2012), The location of reconnection at the magnetopause: Testing the maximum magnetic shear model with THEMIS observations, *J. Geophys. Res.*, *117*, A01201, doi:10.1029/2011JA016959.
Trenchi, L., M. F. Marcucci, G. Pallocchia, G. Consolini, M. B. Bavassano Cattaneo, A. M. Di Lellis, H. Reme, L. Kistler, C. M. Carr, and J. B. Cao (2008), Occurrence of reconnection jets at the dayside magnetopause: Double Star observations, *J. Geophys. Res.*, *113*, A07S10, doi:10.1029/2007JA012774.
Vaivads, A., Y. Khotyaintsev, M. André, A. Retinò, S. C. Buchert, B. N. Rogers, P. Décréau, G. Paschmann, and T. D. Phan (2004), Structure of the magnetic reconnection diffusion region from four spacecraft observations, *Phys. Rev. Lett.*, *93*(10), doi:10.1103/PhysRevLett.93.105001.
Wang, S., L. M. Kistler, C. G. Mouikis, and S. M. Petrinec (2015), Dependence of the dayside magnetopause reconnection rate on local conditions, *J. Geophys. Res. Space Physics*, *120*, 6386–6408, doi:10.1002/2015JA021524.
Zhu, C. B., H. Zhang, Y. S. Ge, Z. Y. Pu, W. L. Liu, W. X. Wan, L. B. Liu, Y. D. Chen, H. J. Le, and Y. F. Wang (2015), Dipole tilt angle effect on magnetic reconnection locations on the magnetopause, *J. Geophys. Res. Space Physics*, *120*, 5344–5354, doi:10.1002/2015JA020989.